OIKOS

The effects of dispersal on spatial synchrony in metapopulations differ by timescale

Journal:	*Oikos*
Manuscript ID	OIK-08298
Wiley - Manuscript type:	Research
Keywords:	metapopulation, dispersal, spatial synchrony, stability, timescale, time series length

Abstract: Dispersal has been well documented to have dual effects by stabilizing and synchronizing local populations, but whether these dispersal effects differ across timescales is largely unknown. Here, we combine a simple metapopulation model and spectral approaches to understand how dispersal affects population variability and spatial synchrony across timescales. Our model shows that dispersal has contrasting effects at short versus long timescales on the variability and synchrony of populations. For populations exhibiting under-compensatory growth (i.e. slow recovery when perturbed), dispersal decreases local population variability and increases spatial synchrony at long timescales, but it increases local population variability and decreases spatial synchrony at short timescales. Thus, the well-known local stabilizing and spatial synchronizing effects of dispersal operate only at long timescales. The contrasting effects of dispersal at short and long timescales lead to a sample size dependency of the empirical relationship between dispersal and population variability or synchrony. Specifically, given sufficiently long time series, spatial synchrony increases, and local population variability decreases, with dispersal. But given short time series, spatial synchrony decreases, and local population variability increases, with dispersal. Our results provide novel insights on the dynamics underlying the role of dispersal and have implications for empirical studies and management of metapopulations.

The effects of dispersal on spatial synchrony in metapopulations differ by timescale

Abstract: Dispersal has been well documented to have dual effects by stabilizing and synchronizing local populations, but whether these dispersal effects differ across timescales is largely unknown. Here, we combine a simple metapopulation model and spectral approaches to understand how dispersal affects population variability and spatial synchrony across timescales. Our model shows that dispersal has contrasting effects at short versus long timescales on the variability and synchrony of populations. For populations exhibiting under-compensatory growth (i.e. slow recovery when perturbed), dispersal decreases local population variability and increases spatial synchrony at long timescales, but it increases local population variability and decreases spatial synchrony at short timescales. Thus, the well-known local stabilizing and spatial synchronizing effects of dispersal operate only at long timescales. The contrasting effects of dispersal at short and long timescales lead to a sample size dependency of the empirical relationship between dispersal and population variability or synchrony. Specifically, given sufficiently long time series, spatial synchrony increases, and local population variability decreases, with dispersal. But given short time series, spatial synchrony decreases, and local population variability increases, with dispersal. Our results provide novel insights on the dynamics underlying the role of dispersal and have implications for empirical studies and management of metapopulations.

Keywords: metapopulation, over-compensatory growth, spatial synchrony, stability, timescale, time series length, under-compensatory growth

Introduction

The field of spatial ecology has highlighted that the fate of a local population may be fundamentally tied to interactions with populations surrounding it. This idea has been formalized in the concept of metapopulation, defined as a collection of spatially separate populations that interact through dispersal (Levins 1969; Hanski 1999). Early conceptualizations of metapopulation theory highlighted that dispersal is central to the stability of metapopulations. For instance, in a stochastic environment where populations fluctuate constantly through time, dispersal can provide stabilizing effects by dampening the temporal variability of individual populations (Briggs & Hoopes 2004). On the other hand, dispersal can also generate synchrony across a metapopulation, such that all populations rise and fall at the same time (Liebhold et al. 2004). Synchronized fluctuations can be destabilizing, even causing increased extinction of the entire metapopulation (Heino et al. 1997; Earn et al. 2000). Consequently, the overall effect of dispersal on metapopulation stability is determined by the balance between its locally stabilizing and spatially synchronizing effects (Higgins 2009; Abbott 2011; Wang et al. 2015; Fox 2017).

The stabilizing and synchronizing effects of dispersal have been shown to depend on endogenous and exogenous factors, particularly the species' intrinsic growth rates and spatial correlation in the environment. The population growth rate determines the ability of a perturbed population to recover to its equilibrium, which thereby influences the level of dispersal needed to stabilize or rescue a local population (Wang et al. 2015; Zelnik et al. 2019). At the landscape level, spatial environmental correlation can drive spatial synchrony via Moran effects (i.e., the temporal correlation of two spatially distributed populations equals the spatial correlation in the environment, Moran 1953). Moran effects can also modulate the

role of dispersal, such that the synchronizing effect of dispersal is relatively weaker in a spatially correlated environment (Kendall et al. 2000; Ripa 2000; Liebhold et al. 2004). Thus, dispersal, local population growth rate, and environmental correlation interact and jointly shape the stability and synchrony in metapopulations (Kendall et al. 2000; Wang et al. 2015). As these factors operate at different timescales (i.e. periods of fluctuations, such as annual or decadal), the combination of these drivers may differentially affect population dynamics and spatial synchrony across timescales.

The timescale-specific patterns of population dynamics have long been acknowledged in ecological studies. Early studies reported that natural populations often exhibit positively autocorrelated temporal dynamics, which means that population dynamics are dominated by fluctuations at long timescales from a spectral perspective (Pimm & Redfearn 1988; Halley 1996; Inchausti & Halley 2001). Understanding the mechanisms underlying these timescale-specific patterns is important because populations with higher temporal autocorrelation are more likely to undergo extinction or regime shifts (Inchausti & Halley 2003; Scheffer et al. 2009; Garcia-Carreras & Reuman 2011). Theoretical models have demonstrated that population growth rate and the timescale structure of environmental fluctuations have significant influence on the timescale-specific patterns of population dynamics (Ripa & Lundberg 1996; Petchey et al. 1997; Kaitala et al. 1997). In particular, populations with low growth rates converge gradually to its equilibrium when perturbed (referred to as “under-compensatory growth”; see Ruokolainen et al. 2009), resulting in population dynamics with positive autocorrelation or characterized by fluctuations at long timescales. In contrast, populations with high growth rates overshoot the equilibrium when perturbed (referred to as “over-compensatory growth”), resulting in

population dynamics with negative autocorrelation or characterized by fluctuations at short timescales. Moreover, the timescale structure of environmental fluctuations can generate similar patterns in population dynamics, e.g. populations living in a positively autocorrelated environment tend to exhibit positive autocorrelation (Kaitala et al. 1997; Garcia-Carreras & Reuman 2011). The effect of the environmental temporal structure also depends on population growth rate, such that environmental autocorrelation impairs (enhances) the persistence of populations with under-compensatory (over-compensatory) growth (Petchey et al. 1997; Ruokolainen et al. 2009).

In a spatial context, the importance of timescale has become evident for understanding synchronous fluctuations of populations across space. Recent theory clarifies that the timescale structure of spatial environmental correlation has strong effects on those of spatial population synchrony (Sheppard et al. 2016; Desharnais et al. 2018). Spatial population synchrony measured at a specific timescale is driven, in part, by spatial environmental correlation at the same timescale. Such an extended, timescale-specific "Moran effect" has provided new opportunities to detect the drivers of spatial population dynamics (Sheppard et al. 2016, 2019; Anderson et al. 2019). For instance, by showing the timescale-specific synchrony of both aphid populations and a number of climatic factors, Sheppard et al. (2016) discovered that winter temperature was also a major Moran driver of the spatial synchrony of aphid phenology. Desharnais et al. (2018) showed that the presence of dispersal could alter the effect of environmental correlation in shaping the timescale-specific patterns of spatial synchrony. Whether dispersal itself affects spatial synchrony differently across different timescales, however, remains an important and understudied problem.

The timescale-specific patterns of population variability and synchrony also have implications for empirical studies. For populations with a positive temporal autocorrelation, a well-documented phenomenon is that the observed temporal variance increases with the length of time series (Pimm & Redfearn 1988; Inchausti & Halley 2002), simply because nearby values tend to be similar and hence short-term variance must be smaller than the long-term one. In contrast, populations with a negative temporal autocorrelation are expected to show lower variance with increasing time series length. Therefore, ecological factors (e.g. dispersal or population growth rate) shaping the timescale-specific patterns of population dynamics can influence the estimate of variability with time series data. Furthermore, if dispersal affect population variability and synchrony differently at different timescales, we expect that the relationships between dispersal and population variability or synchrony may also vary with the length of the time series under investigation. Such dependency on the time series length of empirical studies of metapopulations are particularly relevant for interpreting experimental and observational results.

Here we investigate how dispersal interacts with population growth and the environmental to regulate variability and synchrony at different timescales. With two-patch metapopulation models, we use Fourier transforms to uncover the timescale-specific patterns of population variability and spatial synchrony. We first examine whether dispersal has different effects on population variability or spatial synchrony at short versus long timescales, and test whether these effects differ when populations exhibit under- and over-compensatory growth. We then use simulated time series to investigate relationships of dispersal with population variability and spatial synchrony, and test whether these relationships depend on time series length. Our

analyses derived new predictions on the timescale-dependent effects of dispersal, and we end with discussion on the theoretical and practical implications of our results.

Methods

The metapopulation model

We consider a two-patch discrete-time metapopulation model, in which population dynamics are governed by a Ricker growth function, environmental stochasticity, and dispersal:

$$x_i'(t) = (1-d)\cdot x_i(t) + d\cdot x_j(t) \tag{1a}$$

$$x_i(t+1) = x_i'(t)\cdot \exp\left(r_i\left(1-\frac{x_i'(t)}{K_i}\right)+\varepsilon_i(t)\right) \tag{1b}$$

Here, $x_i(t)$ and $x_i'(t)$ denote the population size in patch i recorded before and after the dispersal process, respectively. K_i and r_i are the carrying capacity and intrinsic growth rate in patch i, and d is the dispersal rate. $\boldsymbol{\varepsilon} = (\varepsilon_1, \varepsilon_2)^T$ is two-dimensional Gaussian noise with component variances 0.01 and correlation coefficient ρ, which describes the response of population growth rate to environmental fluctuations. We calculate population variability and synchrony based on $x_i(t)$ to avoid the immediate influence of dispersal (de Raedt et al. 2019; but see Desharnais et al. 2018). Previous studies that considered both $x_i(t)$ and $x_i'(t)$ showed that these two types of models generated qualitatively similar effects of dispersal on synchrony and variability (Wang et al. 2015).

In our model, we consider the intrinsic growth rates (r_i) to be within the interval $(0, 2)$, such that local populations always have stable equilibria K_i. When $0 < r_i < 1$, a local population exhibits under-compensatory growth and converges monotonically to its steady state when disturbed. When $1 < r_i < 2$, the local population exhibits over-

compensatory growth and oscillates but eventually converges to its steady state when disturbed (Ruokolainen et al. 2009; McCann 2012).

Synchrony and variability: overall and timescale-specific measures

We measure the temporal variability by the squared coefficient of variation (CV^2), i.e. the ratio of temporal variance (var(x)) to the squared mean ($\bar{x}^2$) of population size. Given a time series of metapopulation dynamics, we calculate population variability (V_P) by the average temporal variability of the two local populations, i.e. $V_P = (\mathrm{CV}^2(x_1) + \mathrm{CV}^2(x_2))/2$; we calculate metapopulation variability (V_M) by the temporal variability of total metapopulation size ($V_M = \mathrm{CV}^2(x_1 + x_2)$). The spatial synchrony (ϕ) is defined as the temporal correlation between the two populations (i.e. $\phi = \mathrm{cor}(x_1, x_2)$). To be distinguishable from the timescale-specific metrics below, we refer to these metrics as overall (meta)population variability and overall synchrony.

We then derive the timescale-specific metrics for variability and synchrony based on discrete Fourier transformation (Shumway & Stoffer 2017). Specifically, the sample variance of population i can be decomposed into the sum of timescale-specific terms: $\mathrm{var}(x_i) = \sum_\sigma I_{ii}(\sigma)$, where $I_{ii}(\sigma)$ denotes the power spectrum of time series x_i at the time scale $\sigma \in \left\{\frac{T}{T-1}, \frac{T}{T-2}, \ldots, \frac{T}{2}, T\right\}$ (Zhao et al. 2020), corresponding to the frequency $f = T/\sigma$ in other contexts (Halley 1996). Similarly, the sample covariance between populations i and j could be decomposed into sum of timescale-specific terms: $\mathrm{cov}(x_i, x_j) = \sum_\sigma I_{ij}(\sigma)$, where $I_{ij}(\sigma)$ denotes the cospectrum between the time series x_i and x_j. For a timescale σ, we define $V_P(\sigma) = \frac{1}{2}\left(\frac{I_{11}(\sigma)}{\bar{x}_1^2} + \frac{I_{22}(\sigma)}{\bar{x}_2^2}\right)$ as the timescale-specific measure of population variability, and $V_M(\sigma) = \frac{(I_{11}(\sigma)+I_{22}(\sigma)+2I_{12}(\sigma))}{(\bar{x}_1+\bar{x}_2)^2}$ as the timescale-specific measure of metapopulation variability.

By definition, the overall population and metapopulation variability can be expressed as the sum of timescale-specific population and metapopulation variability, respectively, i.e. $V_P = \sum_\sigma V_P(\sigma)$ and $V_M = \sum_\sigma V_M(\sigma)$. We also define $\phi(\sigma) = \frac{I_{12}(\sigma)}{\sqrt{I_{11}(\sigma) \cdot I_{22}(\sigma)}}$ as a timescale-specific measure of synchrony used by Desharnais et al. (2018). The denominator of this metric serves to normalize by the power spectrum of the two time series, so $\phi(\sigma)$ is a timescale-specific measure of synchrony that is independent of timescale-specific patterns of variance (Desharnais et al. 2018). Note that the sum of $\phi(\sigma)$ across timescales does not lead to the overall synchrony ϕ.

Analytic investigation

We solve analytically our model (1) in a spatially homogeneous case, i.e. the two patches have same environmental conditions ($r_1 = r_2 = r, K_1 = K_2 = K$), using a linearization approximation (Appendix B). For the overall metrics of variability and synchrony, previous studies have provided analytic solutions for ϕ, V_P, and V_M (Abbott 2011; Wang et al. 2015). These solutions show that dispersal decreases the variability of local populations but increases spatial synchrony; these two effects cancel out at the larger metapopulation scale, such that dispersal has no effect on the stability of the metapopulation. Given the homogeneity assumption of our model, we also have: $V_M = V_P \cdot (1 + \phi)/2$ (Wang et al. 2015). For the timescale-specific metrics, we can similarly linearize the model and use filter theory of time series (Reinsel 1993) to derive the analytic solutions for $\phi(\sigma)$, $V_P(\sigma)$, and $V_M(\sigma)$ as functions of timescale, growth rate, dispersal and timescale-specific variance/synchrony of environmental noise (Appendix B; see also Desharnais et al. 2018). We note that the analytical solutions of timescale-specific variability and synchrony correspond to Fourier transforms of infinite time series (Appendix B). To visualize and compare with simulation results

197 based on finite time series of length L, we rescaled the timescale-specific variability
198 and synchrony by: $z'(\sigma) = \frac{z(\sigma)}{L}$, where $z(\sigma)$ denotes $\phi(\sigma)$, $V_P(\sigma)$, or $V_M(\sigma)$
199 (Appendix A).
200
201 ***Simulations***
202 We first simulated the nonlinear dynamics described by eqn. (1) in homogenous
203 landscapes with the same values of r and K in the two patches. We did so across a
204 range of parameter values, systematically varying intrinsic growth rate ($r =$
205 $0.45, 0.55, \ldots, 1.55$), dispersal ($d = 0, 0.05, 0.1, \ldots 0.5$), and spatial correlation in the
206 environment ($\rho = 0, 0.1, \ldots, 0.9$). For each set of parameters, we set the initial values
207 of population sizes as the carrying capacities K and ran the simulations for 1000 time
208 steps to ensure that populations reach their stationary states and then recorded time
209 series of the following 200 time steps. With the simulated time series, we applied the
210 discrete Fourier transform (using the function "fft" in Matlab) to derive the timescale
211 specific metrics of variability and synchrony.
212 The length of time series may affect our ability to detect timescale-specific patterns
213 of variability and synchrony and their relation with ecological factors (Inchausti &
214 Halley 2002). To investigate this, we simulated metapopulation dynamics to stationary
215 states ($T = 1000$) and then record time series with different lengths or number of time
216 steps. We examined how the empirical estimates of overall variability and synchrony
217 change with the time series length. We also examined how the "observed" relationships
218 (i.e. based on our simulated data) between dispersal and overall synchrony or variability
219 might differ between short (5 timesteps) and long (60) time series.
220 We then performed further simulations to test whether our results hold in
221 landscapes with spatial heterogeneity, temporally autocorrelated environmental noises,

and more patches. We first simulated heterogeneous metapopulations with asymmetric population growth rates ($r_1 \neq r_2$) or carrying capacity ($K_1 \neq K_2$). We then consider cases where the environmental noise is temporally autocorrelated. Specifically, we define the noise term by a first-order autoregressive process (AR(1)): $\varepsilon_i(t) = q\varepsilon_i(t-1) + \xi_i(t)$, where $\xi_i(t)$ are white noises and $0 \leq q < 1$, $i = 1,2$. A larger autoregression coefficient q will result in a higher temporal autocorrelation. Lastly, we simulated a 16-patch metapopulation model with local population growth characterized by eqn (1b) and global dispersal, i.e. an emigrant from one patch has equal probabilities of immigrating into the other 15 patches.

Results

Analytic approximations for homogeneous metapopulations

We derive analytic solutions for timescale-specific metrics of synchrony and variability in homogenous landscapes (Appendix B). In the case that the environmental noise has the same power spectrum (I_0) and spatial synchrony (ρ) at all timescales, the timescale-specific solutions for spatial synchrony ($\phi(\sigma)$), population variability ($V_P(\sigma)$) and metapopulation variability ($V_M(\sigma)$) can be simplified as (Appendix B, eqn. B14 to B16):

$$\phi(\sigma) = \frac{(1-\alpha)\rho+\alpha}{(1-\alpha)+\alpha\rho} \quad (2)$$

$$V_P(\sigma) = \frac{[(1-\alpha)+\alpha\rho]\cdot I_0}{1+(1-r)^2-2(1-r)\cdot\cos(2\pi/\sigma)} \quad (3)$$

$$V_M(\sigma) = \frac{1}{2}\cdot\frac{(1+\rho)\cdot I_0}{1+(1-r)^2-2(1-r)\cdot\cos(2\pi/\sigma)} \quad (4)$$

where $\alpha(\sigma) = \frac{2d(1-r)(\cos(2\pi/\sigma)-(1-d)(1-r))}{((1-2d)(1-r))^2+2(1-2d)(1-r)\cdot\cos(2\pi/\sigma)+1}$.

The above solutions clarify how the timescale-specific patterns of synchrony and variability depend on population dynamical parameters. In particular, the timescale-specific variability for both local populations and metapopulations increase as the

timescale (σ) increases when population dynamics are under-compensatory ($r < 1$), and they both decrease as σ increases when population dynamics are over-compensatory ($r > 1$) (Fig. 1; Appendix B). Similarly, at short timescales, synchrony and both population and metapopulation variability all increase as r increases; at long timescales, all these synchrony and variability metrics decrease as r increases (Fig. 1; Appendix B).

The effect of dispersal on synchrony and variability depends on the timescale considered and the population growth rate (Fig. 2). When $r < 1$, dispersal increases spatial synchrony and decreases population variability at long timescales, but it has just the inverse effects at short timescales. When $r > 1$, dispersal has the opposite effects on spatial synchrony and population variability at both short and long timescales. In the absence of dispersal, spatial synchrony equals ρ at all timescales (Fig. 2b,e), as expected from the timescale-specific Moran's theorem (Desharnais et al. 2018). Besides, dispersal has no effect on the metapopulation variability at all timescales (Fig. 2c,f).

The correlation of environmental noises (ρ) has positive effect on spatial synchrony and metapopulation variability at all timescales, regardless of the magnitude of r (Fig. D1). But the effects of environmental correlation on local population variability differ between under- and over-compensatory systems (Fig. D1). When $r < 1$, local population variability increases as ρ increases at long timescales, but it decreases slightly as ρ increases at short timescales. When $r > 1$, the opposite is true. See Appendix B for analytic investigations on the dependency of V_P, ϕ and V_M on parameters d, σ and ρ.

Variability and synchrony in simulated metapopulations

Our simulations of homogeneous metapopulations reveal similar patterns as the

271 analytic solutions, provided sufficiently long time series (e.g. 200 timesteps). In
272 particular, dispersal has contrasting effects on variability and synchrony at short and
273 long timescales, which depend on whether population growth follows under- or over-
274 compensatory dynamics. In under-compensatory systems ($r < 1$), spatial synchrony
275 increases, and population variability decreases, as dispersal increases, at long
276 timescales; in contrast, spatial synchrony decreases, and population variability
277 increases, as dispersal decreases, at short timescales (Fig. D2a,b). In over-compensatory
278 systems ($r > 1$), the effects of dispersal are opposite at both short and long timescales
279 (Fig. D2d,e). In these homogeneous metapopulations, dispersal has no effect on
280 metapopulation variability at all timescales, regardless of r (Fig. D2c,f). Besides, the
281 (meta)population variability and synchrony all increase with r at short timescales, and
282 they decrease with r at long timescales (Fig. D3). The environmental correlation
283 generally increases metapopulation variability and synchrony, except for population
284 variability at short timescales when $r < 1$, or at long timescales when $r > 1$ (Fig. D1
285 g,j). All these effects of dispersal, growth rate, and environmental correlation are
286 consistent with analytic solutions (Figs. 1, 2, D1-D3).

287 We then explore how the length of time series may influence the empirical
288 estimates of the overall spatial synchrony and overall (meta)population variability, as
289 well as their relationships with dispersal and intrinsic growth rate. Our results show that
290 the overall variability of local populations and metapopulations both increase with time
291 series length in under-compensatory systems ($r < 1$), but they decrease with time series
292 length in over-compensatory systems ($r > 1$) (Fig. D4). The former pattern (i.e. when
293 $r < 1$) is consistent with previous empirical studies (Pimm & Redfearn 1988; Inchausti
294 & Halley 2002). These patterns are robust in the presence or absence of dispersal. We
295 also found that the overall spatial synchrony increases with time series length when

296 $r < 1$, but it does not change significantly when $r > 1$ (Fig. D4). Note, however, in
297 the absence of dispersal ($d = 0$), the sample synchrony is always close to zero,
298 regardless of time series length (Fig. D4).

299 Furthermore, the length of time series used for calculations directly influence the
300 empirical relationship between dispersal and overall synchrony or population
301 variability, even though the time series are generated from the same underlying model
302 and only differ in their length. Specifically, given a long time series (length = 60), the
303 overall synchrony increases, and overall population variability decreases, as dispersal
304 increases, no matter whether local populations exhibit under- or over-compensatory
305 dynamics (Fig. 3d,e). However, given a short time series (length = 5), the overall spatial
306 synchrony decreases, and the overall population variability increases, as dispersal
307 increases, when populations exhibit under-compensatory growth (i.e. $r < 1$); opposite
308 patterns are observed when populations exhibit over-compensatory growth (i.e. $r > 1$)
309 (Fig. 3a,b). In other words, when populations exhibited under-compensatory dynamics,
310 dispersal has contrasting effects on spatial synchrony or population variability in short
311 versus long time series. Lastly, the metapopulation variability exhibits no relation with
312 dispersal, regardless of the time series length or whether populations follow under- or
313 over-compensatory dynamics (Fig. 3c,f).

314 Similarly, the overall synchrony or (meta)population variability also exhibit
315 contrasting relationships with the intrinsic growth rate (r) in short versus long time
316 series. Given a long time series (length = 60), the overall synchrony and
317 (meta)population variability all exhibit U-shape curves with r (Fig. D5), consistent
318 with theoretical predictions (Wang et al. 2015). However, given a short time series
319 (length = 5), the overall synchrony and (meta)population variability all increase
320 monotonically with r (Fig. D5). Besides, the overall synchrony and (meta)population

variability generally exhibit positive relationships with the environmental correlation, except that the variability of under-compensatory populations decreases slightly with ρ in short time series (Fig. D6).

To examine how additional ecological complexity alter the above results obtained from homogeneous metapopulations with white noises, we simulate population dynamics in heterogeneous landscapes or in temporally autocorrelated environments (Fig. 4). In heterogeneous landscapes where the two patches differ in their intrinsic growth rates (r) or carrying capacities (K), spatial synchrony generally increase as dispersal increases in over-compensatory systems ($r > 1$); in under-compensatory systems ($r < 1$), spatial synchrony decreases as dispersal increases in short time series, and it increased as dispersal increases in long time series (Fig. 4). Such patterns also hold if the environmental fluctuations exhibited temporal autocorrelation. That said, if the environmental autocorrelation is very strong, spatial synchrony always increases with dispersal, regardless of the time series length (Fig. 4). Besides, our simulations using 16-patch models exhibited similar time length dependency of spatial asynchrony-dispersal relationship as 2-patch ones (Fig. D8). In all these heterogenous or autocorrelated scenarios, the overall population variability exhibits opposite patterns compared to those of overall synchrony (Fig. D7, D8). Overall, we find our results for 2-patch homogeneous metacommunities with white noise are generally consistent across larger or heterogeneous metacommunities or with temporally autocorrelated environmental variability.

Discussion

Our study demonstrates, to our knowledge for the first time, that dispersal has contrasting effects on spatial synchrony and population variability at short versus long

timescales. In particular, we show that the well-documented locally stabilizing and spatially synchronizing effects of dispersal operate only at particular timescales, and opposite effects can arise at other timescales. We present analytic predictions for homogenous systems, which are shown by simulations to hold in broader context with spatial heterogeneity and environmental autocorrelation. One implication of the timescale-dependent effects of dispersal is that the empirical relationship between dispersal and spatial synchrony or population variability can exhibit opposite patterns, simply because of different time series lengths. Our findings have direct implications for experimental and observational studies to understand the role of dispersal in metapopulation dynamics.

Contrasting effects of dispersal at short versus long timescales

The effects of dispersal on population variability and synchrony have been widely explored in metapopulation models. Previous models showed that dispersal is a 'double-edged sword' for metapopulation stability by decreasing local population variability but meanwhile increasing spatial synchrony (Hudson & Cattadori 1999; Kendall et al. 2000; Abbott et al. 2011; Wang et al. 2015). While such local stabilizing and spatially synchronizing effects of dispersal are intuitive and well understood, our model demonstrates that these two effects are timescale-dependent and, moreover, such timescale-dependency relies on the nature of population growth of the species of interest.

For populations exhibiting under-compensatory growth (i.e. monotonic recovery when perturbed), the local stabilizing and spatially synchronizing effects of dispersal operate mainly at long timescales. At short timescales, counterintuitively, dispersal destabilizes local populations and desynchronizes population dynamics across patches.

Such counterintuitive effects can be understood from the interaction between random fluctuations and the statistical averaging effect of dispersal (Briggs & Hoopes 2004). More specifically, consider a starting point where the two patches have different population sizes due to environmental fluctuations. During the next step, dispersal will decrease the population size in one patch and increase it in the other, followed by relatively moderate changes in population size driven by local under-compensatory population growth in both patches (Fig. 5). Therefore, in the short run, dispersal causes different population sizes to converge toward intermediate values, which generates a negative correlation between populations and thus decreases spatial synchrony (Fig. 5). In contrast, for populations exhibiting over-compensatory growth (i.e. oscillatory recovery when perturbed), the timescale-dependency of dispersal is opposite, i.e. dispersal has local stabilizing and spatially synchronizing effects at short timescales, and opposites effects at long timescales. Despite the contrasting effects of dispersal across timescales, dispersal always increases the overall spatial synchrony in both under- and over-compensatory populations (Fig. 3; see also Abbott 2011; Wang et al. 2015). This is because the synchronizing effects of dispersal occur at the same timescale that dominate population dynamics, i.e. the long (short) timescales for under- (over-) compensatory dynamics (Figs. 2&3).

Although previous studies revealed both under- and over-compensatory growth in natural populations, the former was found to be much more common than the latter (Fagan et al. 2010; Cortes 2016). In these under-compensatory populations, the contrasting effects of dispersal at short versus long timescales lead to an increasing trend of spatial synchrony with timescales, even if spatial environmental correlation is constant at all timescales (Fig. 2). Such an increasing trend of spatial synchrony with timescale is consistent with observations from recent empirical studies, which revealed

a higher spatial asynchrony at longer timescales in gypsy moth defoliation (Walter et al. 2017), zooplankton abundances (Anderson et al. 2019), and the productivity of terrestrial vegetation and marine phytoplankton (Defriez & Reuman 2017a, 2017b; Sheppard et al. 2019). These studies suggested that the higher spatial synchrony at longer timescales might be attributed to a stronger spatial environmental correlation at long timescales (Sheppard et al. 2015, 2019; Desharnais et al. 2018). Our theoretical results provide an alternative explanation from endogenous processes, i.e. the interaction between dispersal and under-compensatory dynamics.

Time series length matters in metapopulation studies

The contrasting effects of dispersal at short versus long timescales lead to a sample size dependency of the empirical relationship between dispersal and population variability or synchrony. For populations with under-compensatory growth, short time series would reveal a positive effect of dispersal on the overall population variability and a negative effect on overall spatial synchrony, which is the opposite of predictions derived from long time series or analytic solutions (Fig. 3; Abbott 2011; Wang et al. 2015). Such a contrast is explained by the fact that short time series represented information mainly at short timescales, at which dispersal has opposite effects from long timescales (Fig. 5). In comparison, long time series cover information at both short and long timescales, which reflect the combined effect of dispersal across all timescales. Such a sample size dependency also applies to other factors that exhibits contrasting effects at short and long timescales, for instance population growth rate (Fig. D5).

Such a sample size dependency has two implications for ecological research. First, to understand the effect of dispersal (and other factors), comparison between metapopulation experimental studies should be made among experiments with similar

time series length and between species with similar types of growth (e.g. over- or under-compensatory). A growing number of metapopulation experiments has been conducted to test the effect of dispersal on spatial synchrony and population variability, which revealed a range of effect sizes and directions (Dey & Joshi 2006; Steiner et al. 2011, 2013, Thompson et al. 2014). Our results suggest that different time series length might complicate across-study comparison and account for the idiosyncratic conclusions in the literature. For instance, Smeti et al. (2016) conducted an experiment of phytoplankton metapopulations that spanned 15-30 generations and found no significant effects of dispersal on spatial asynchrony. Our results suggested that the short experimental period may explain such insignificant effect of dispersal. Second, because the goal of understanding variability and synchrony is to eventually predict the long-term persistence of populations, we argue that sufficiently long time series should be used to reveal the long-term, or "theoretically expected", relationship between dispersal and population dynamics. An important question remains: "How long will it take for experimental research to reveal the "theoretically expected" relationship?

Determining the 'critical length' is particularly useful for metapopulation study design as well as cross-study comparisons. We suggest that a tentative time series length may be derived by conducting a simulation-based statistical power analysis. Specifically, based on prior knowledge on the dynamical parameters of the focal species (e.g. intrinsic growth rate), one can simulate metapopulation models with different experimental setting (e.g. gradients of dispersal, environmental noise, number of replicates, etc.) and numerically determine the minimum time series length for exhibiting a positive dispersal-spatial synchrony relationship with a given accuracy (Appendix C). Our preliminary analyses show that a longer time series or more replicates are required for metapopulations with under-compensatory dynamics ($r <$

1), a lower environmental correlation between patches and replicates (ρ), and a narrower gradient of dispersal rate, whereas the variance of environmental noise (σ^2) has only moderate influence (Fig. C3). We encourage such kind of power analysis before starting a metapopulation study or doing meta-analyses on such studies.

Conclusion

The past decades of metapopulation research have made significant progress in understanding the role of dispersal in population variability and synchrony. To date, however, studies have generally used overall measures of variability and synchrony that integrate information over a wide range of timescales, which potentially overlooked the timescale dependence of dispersal effects. Our study demonstrates that dispersal has contrasting effects on population variability and synchrony at short versus long timescales. Such a timescale-specific perspective not only provides a new look on the dynamics underlying the role of dispersal in metapopulations, but also has important implications for how we interpret the results from empirical studies utilizing time series of different lengths. Our study highlights the importance of accounting for the temporal scale when comparing results among studies of spatial synchrony. This is in line with recent calls to account for spatial scale when comparing results among studies of biodiversity and stability (Chase & Knight 2013; Wang et al. 2017). Our findings add to a growing body of work supporting the idea that long-term, continual data collection (e.g. the long-term ecological research; LTER) is needed to advance population ecology (Clutton-Brock and Sheldon 2010; Gaiser et al. 2020).

Reference

471 Abbott, K. C. 2011. A dispersal-induced paradox: synchrony and stability in
472 stochastic metapopulations: Dispersal-induced paradox in metapopulations.
473 Ecology Letters 14:1158–1169.
474 Anderson, T. L., et al. 2019. The dependence of synchrony on timescale and
475 geography in freshwater plankton. Limnology and Oceanography 64:483–502.
476 Bloomfield, P., 2004. Fourier analysis of time series: an introduction. John Wiley &
477 Sons. New York.
478 Briggs, C. J., and M. F. Hoopes. 2004. Stabilizing effects in spatial parasitoid–host
479 and predator–prey models: a review. Theoretical Population Biology 65:299–315.
480 Brillinger, D. R., 2001. Time series: data analysis and theory. Society for Industrial
481 and Applied Mathematics. San Francisco.
482 Chase, J. M., and T. M. Knight. 2013. Scale-dependent effect sizes of ecological
483 drivers on biodiversity: why standardised sampling is not enough. Ecology
484 Letters 16:17–26.
485 Clutton-Brock, T., and B. C. Sheldon. 2010. Individuals and populations: the role of
486 long-term, individual-based studies of animals in ecology and evolutionary
487 biology. Trends in Ecology & Evolution 25:562–573.
488 De Raedt, J., J. M. Baert, C. R. Janssen, and F. De Laender. 2019. Stressor fluxes alter
489 the relationship between beta-diversity and regional productivity. Oikos
490 128:1015–1026.
491 Defriez, E. J., and D. C. Reuman. 2017a. A global geography of synchrony for marine
492 phytoplankton. Global Ecology and Biogeography 26:867–877.
493 Defriez, E. J., and D. C. Reuman. 2017b. A global geography of synchrony for
494 terrestrial vegetation. Global Ecology and Biogeography 26:878–888.
495 Desharnais, R. A., D. C. Reuman, R. F. Costantino, and J. E. Cohen. 2018. Temporal

scale of environmental correlations affects ecological synchrony. Ecology Letters 21:1800–1811.

Earn, D., S. Levin., and P. Rohani. 2000. Coherence and conservation. Science 290:1360–1364.

Fox, J. W., D. Vasseur, M. Cotroneo, L. Guan, and F. Simon. 2017. Population extinctions can increase metapopulation persistence. Nature Ecology & Evolution 1:1271–1278.

Gaiser, E. E., et al. 2020. Long-Term Ecological Research and Evolving Frameworks of Disturbance Ecology. BioScience 70:141–156.

García-Carreras, B., and D. C. Reuman. 2011. An empirical link between the spectral colour of climate and the spectral colour of field populations in the context of climate change: Climate and population spectral colours. Journal of Animal Ecology 80:1042–1048.

Halley, J. M. 1996. Ecology, evolution and 1f noise. Trends in Ecology & Evolution 11:33–37.

Hanski, I. 1999. Metapopulation ecology. Oxford University Press. Oxford.

Heino, M., V. Kaitala, E. Ranta, and J. Lindström. 1997. Synchronous dynamics and rates of extinction in spatially structured populations. Proceedings of the Royal Society of London. Series B: Biological Sciences 264:481–486.

Higgins, K. 2009. Metapopulation extinction risk: Dispersal's duplicity. Theoretical Population Biology 76:146–155.

Hudson, P. J., and I. M. Cattadori. 1999. The Moran effect: a cause of population synchrony. Trends in Ecology & Evolution 14:1–2.

Inchausti, P., and J. M. Halley. 2001. Investigating Long-Term Ecological Variability Using the Global Population Dynamics Database. Science 293:655–657.

521 Inchausti, P., and J. M. Halley. 2002. The long-term temporal variability and spectral
522 colour of animal populations. Evolutionary Ecology Research 4:1033–1048.
523 Inchausti, P., and J. M. Halley. 2003. On the relation between temporal variability and
524 persistence time in animal populations. Journal of Animal Ecology 72:899–908.
525 Kaitala, V., J. likarjula, E. Ranta, and P. Lundberg. 1997. Population dynamics and
526 the colour of environmental noise. Proceedings of the Royal Society of London.
527 Series B: Biological Sciences 264:943–948.
528 Kendall, B. E., O. N. Bjørnstad, J. Bascompte, T. H. Keitt, and W. F. Fagan. 2000.
529 Dispersal, Environmental Correlation, and Spatial Synchrony in Population
530 Dynamics. The American Naturalist 155:628–636.
531 Levins, R. 1969. Some Demographic and Genetic Consequences of Environmental
532 Heterogeneity for Biological Control. Bulletin of the Entomological Society of
533 America 15:237–240.
534 Liebhold, A., W. D. Koenig, and O. N. Bjørnstad.2004. Spatial Synchrony in
535 Population Dynamics. Annual Review of Ecology, Evolution, and Systematics
536 35:467–490.
537 McCann, K. S. 2012. Food webs, Monographs in population biology. Princeton
538 University Press, Princeton, N.J.
539 Moran, P. 1953. The statistical analysis of the Canadian Lynx cycle. Australian
540 Journal of Zoology 1:291–298.
541 Murray, J. D. 2002. Mathematical biology, 3rd ed. Interdisciplinary applied
542 mathematics. Springer, New York.
543 Petchey, O. L., A. Gonzalez, and H. B. Wilson. 1997. Effects on population
544 persistence: the interaction between environmental noise colour, intraspecific
545 competition and space. Proceedings of the Royal Society of London. Series B:

546 Biological Sciences 264:1841–1847.
547 Pimm, S. L., and A. Redfearn. 1988. The variability of population densities. Nature
548 334:613–614.
549 Reinsel, G. C. 1993. Elements of Multivariate Time Series Analysis, Springer Series
550 in Statistics. Springer US, New York, NY.
551 Ripa, J. 2000. Analysing the Moran effect and dispersal: their significance and
552 interaction in synchronous population dynamics. Oikos 89:175–187.
553 Ripa, J., and P. Lundberg. 1996. Noise colour and the risk of population extinctions.
554 Proceedings of the Royal Society of London. Series B: Biological Sciences
555 263:1751–1753.
556 Ruokolainen, L., A. Lindén, V. Kaitala, and M. S. Fowler. 2009. Ecological and
557 evolutionary dynamics under coloured environmental variation. Trends in
558 Ecology & Evolution 24:555–563.
559 Scheffer, M., et al. 2009. Early-warning signals for critical transitions. Nature
560 461:53–59.
561 Sheppard, L. W., J. R. Bell, R. Harrington, and D. C. Reuman. 2016. Changes in
562 large-scale climate alter spatial synchrony of aphid pests. Nature Climate Change
563 6:610–613.
564 Sheppard, L. W., E. J. Defriez, P. C. Reid, and D. C. Reuman. 2019. Synchrony is
565 more than its top-down and climatic parts: interacting Moran effects on
566 phytoplankton in British seas. PLOS Computational Biology 15:e1006744.
567 Shumway, R. H., and D. C. Stoffer. 2017. Time Series Analysis and Its Applications:
568 With R Examples, Springer Texts in Statistics. Springer International Publishing,
569 Cham.
570 Smeti, E., D. L. Roelke, and S. Spatharis. 2016. Spatial Averaging and Disturbance

571 Lead to High Productivity in Aquatic Metacommunities. Oikos 125, 812–820.
572 Steiner, C. F., R. D. Stockwell, V. Kalaimani, and Z. Aqel. 2011. Dispersal Promotes
573 Compensatory Dynamics and Stability in Forced Metacommunities. The
574 American Naturalist 178:159–170.
575 Steiner, C. F., R. D. Stockwell, V. Kalaimani, and Z. Aqel. 2013. Population
576 synchrony and stability in environmentally forced metacommunities. Oikos
577 122:1195–1206.
578 Thompson, P. L., B. E. Beisner, and A. Gonzalez. 2015. Warming induces synchrony
579 and destabilizes experimental pond zooplankton metacommunities. Oikos
580 124:1171–1180.
581 Walter, J. A., et al. 2017. The geography of spatial synchrony. Ecology Letters
582 20:801–814.
583 Wang, S., B. Haegeman, and M. Loreau. 2015. Dispersal and metapopulation
584 stability. PeerJ 3:e1295.
585 Wang, S., et al. 2017. An invariability-area relationship sheds new light on the spatial
586 scaling of ecological stability. Nature Communications 8:15211.
587 Zelnik, Y. R., J. Arnoldi, M. Loreau. 2019. The three regimes of spatial recovery.
588 Ecology 100:e02586.
589 Zhao, L., et al. 2020. A new variance ratio metric to detect the timescale of
590 compensatory dynamics. Ecosphere 11:e03114.
591

592 **Figure 1.** Timescale-specific population variability ($V_P(\sigma)$, a), spatial synchrony ($\phi(\sigma)$,
593 b) and metapopulation variability ($V_M(\sigma)$, c) as functions of timescale ($2 \leq \sigma \leq 100$)
594 and growth rate (r), derived from analytic approximations. Parameters: $\rho = 0, d =$
595 $0.2, K = 10, \text{var}(\epsilon) = 0.01$.
596 **Figure 2.** Timescale-specific population variability ($V_P(\sigma)$), spatial synchrony ($\phi(\sigma)$)
597 and metapopulation variability ($V_M(\sigma)$) as functions of timescale and dispersal rate (d),
598 derived from analytic approximations. Note that spatial synchrony always equals 0
599 when d = 0, which is invisible in the figure. Parameters are set with $r = 0.5$ (under-
600 compensatory, a,b,c), 1.5 (over-compensatory, d,e,f), and $\rho = 0, K = 10$, $\text{var}(\epsilon) =$
601 0.01.
602 **Figure 3.** Effect of dispersal on local population variability (a,d), spatial synchrony
603 (b,e), and metapopulation variability (c,f) calculated from short (a,b,c) and long (d,e,f)
604 time series. Blue and red lines represent models with under- and over-compensatory
605 population growth ($r = 0.5$ or 1.5), respectively. Dash lines represent respectively
606 analytical solutions of variability & synchrony derived in Wang et al. (2015) (note that
607 solutions are the same when $r = 0.5$ and 1.5). Parameters: $\rho = 0, \text{var}(\epsilon) = 0.1, K =$
608 10. The results represent the average across 500000 (length=5) or 50000 (length=60)
609 simulated communities.
610 **Figure 4.** Effect of dispersal on spatial synchrony calculated from short (a,b,c,d), and
611 long (e,f,g,h) time series under four scenarios: spatial heterogeneity in the intrinsic rate
612 of under-compensatory grown (a,e), spatial heterogeneity in the intrinsic rate of over-
613 compensatory grown (b,f), spatial heterogeneity in the carrying capacity (c,g), and
614 temporally autocorrelated environmental noise (i.e. red noise; d,h). Parameters are set
615 as follows when not specified: $\rho = 0$, $\text{var}(\epsilon) = 0.1$, r = 0.5 $K = 10$. The results
616 represent the average across 500000 (length=5) or 50000 (length=60) simulated

617 communities.

618 **Figure 5.** An illustration on the dispersal-induced negative synchrony at short
619 timescales in under-compensatory systems: with (a-c) and without (d-f) dispersal. Each
620 panel represents the dynamics of two populations (blue and red) during one time step.
621 Three different scenarios of the initial states are shown in (a,d), (b,e) and (c,f). Starting
622 from a different population size (i.e. $x_1(t)$ and $x_2(t)$), each population experiences first
623 dispersal (d) and then local growth (r), indicated by the thick and thin arrows,
624 respectively. The dashed lines indicate the overall changes during one time step. Strong
625 dispersal reduces the difference between the two populations via a statistical averaging
626 effect, and then the intrinsic growths moves the population size towards the equilibrium.
627 Note that in a highly under-compensatory systems, the effects of intrinsic growth are
628 moderate in one time step. Overall, the two populations always exhibit a negative
629 correlation during one time step (between t and t+1) in the presence of dispersal (a-c),
630 and either positive (e,f) or negative (d) correlations in the absence of dispersal.

631

632 **Figure 1.**

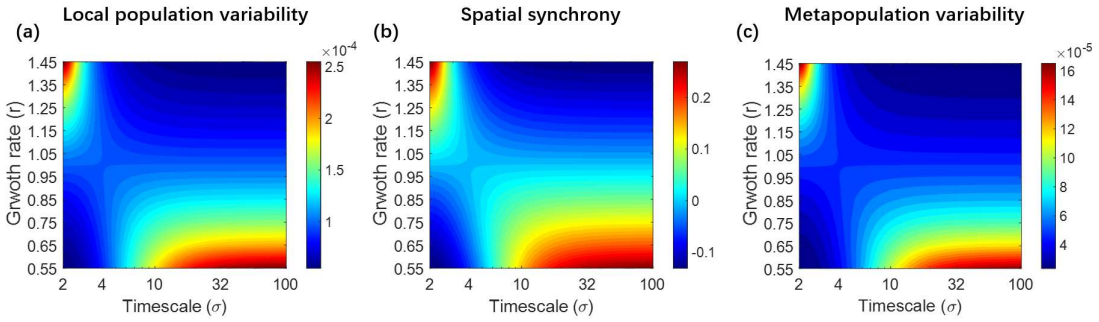

633

634

635 **Figure 2.**

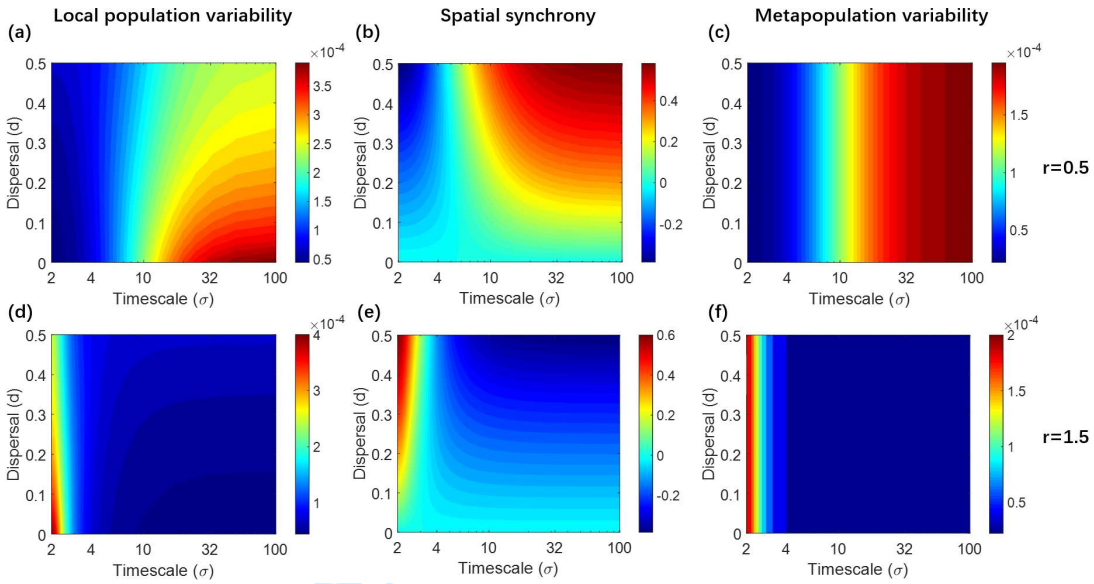

636

637

638 **Figure 3.**

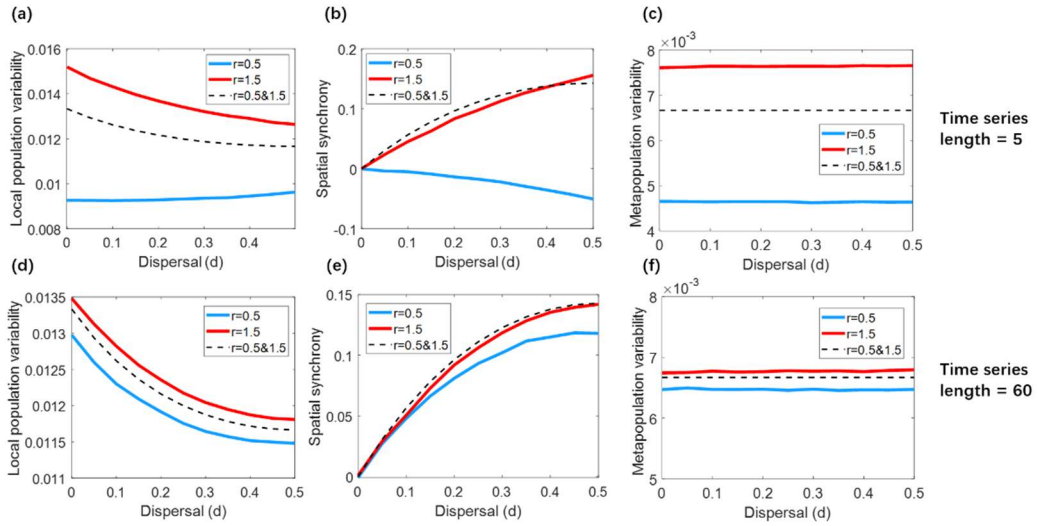

639

640

641 **Figure 4.**

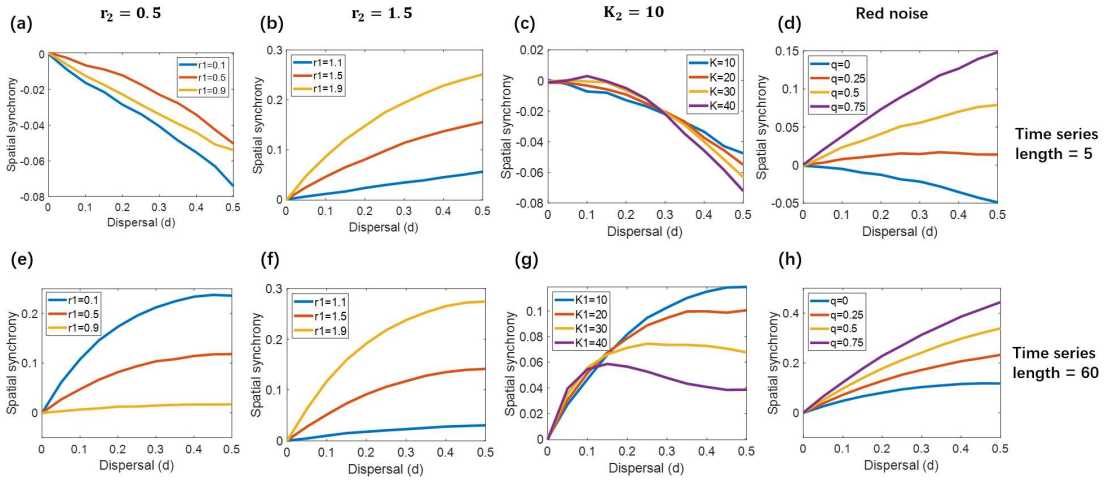

642

643

644 **Figure 5.**

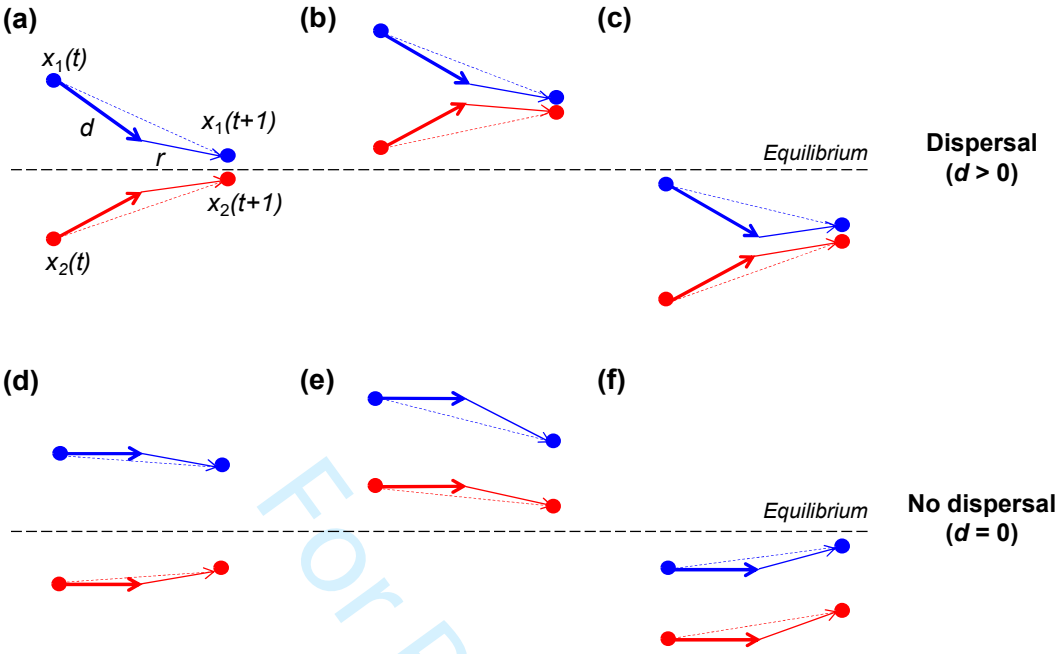

645

Supplementary Information for

The effects of dispersal on spatial synchrony in metapopulations differ by timescale

s

Appendix A. Details of timescale approaches of variability/synchrony analysis

The discrete Fourier transform of data $\{x(t)\}_{t=1}^{T}$ is defined as

$$U_x(f) = \sum_{t=1}^{T} x(t) \cdot \omega_T^{f(t-1)}, f = 1,2,...,T-1$$

where $\omega_T = \exp(-2\pi i/T)$. The power spectrum is

$$I_{xx}(f) = \frac{|U_x(f)|^2}{T(T-1)}$$

And the co-spectrum (real part of cross spectrum) of two time series $x(t)$ and $y(t)$ is defined as

$$I_{xy}(f) = \frac{\mathrm{Re}\left(U_x(f) \cdot \overline{U_y(f)}\right)}{T(T-1)}$$

Parseval's formula gives $\sum_{f=1}^{T-1} I_{xx}(f) = \mathrm{var}(x)$ and $\sum_{f=1}^{T-1} I_{xy}(f) = \mathrm{cov}(x,y)$. The notation "var" and "cov" here stand for sample variance and covariance (Bloomfield 2004, section 10.2).

The frequency f (units of cycles per T sampling intervals) can be transformed into timescale σ via:

$$\sigma = T/f$$

with $f = 1,2,...,T-1$. Note that $U(f) = U(T-f)$.

Reference

Bloomfield, P., 2004. Fourier analysis of time series: an introduction. John Wiley & Sons. New York.

Appendix B. Theoretical analysis of the linearized metapopulation model

Following the analytical approach in the supporting information of Desharnais et al. (2018), we will study a local linearization (Taylor expansion of order 1, Murray 2002, chapter 2 and 3 of vol. 1) of our two-patch Ricker model in the main text (1a) and (1b) at the equilibrium point $(x_1,x_2) = (K, K)$ and solve the timescale specific variability and synchrony of the linearized model. The matrix form of the linearized model is

$$\boldsymbol{w}(t) = c\begin{bmatrix} 1-d & d \\ d & 1-d \end{bmatrix}\boldsymbol{w}(t-1) + \boldsymbol{\xi}(t) \quad \text{(B1)}$$

where $\boldsymbol{w}(t) = (w_1(t),w_2(t))^T$ with $w_i(t) = x_i(t) - K$ $(i = 1,2)$ denoting the local fluctuation of population size, and $c = 1 - r$ is the measurement of population regulation around equilibrium. It can be found that the system with $d = 0$ is locally stable when $-1 < c < 1$, i.e. $0 < r < 2$. When $0 < c < 1$ (i.e. $0 < r < 1$), the individual habitat patches are under-compensatory, i.e., the population abundance will converge to its equilibrium monotonically when disturbed locally. When $-1 < c < 0$ (i.e. $1 < r < 2$), the individual patches are over-compensatory, i.e., the population abundances will converge in an oscillatory manner to the equilibrium when disturbed locally. The linearized random term $\boldsymbol{\xi} = (\xi_1,\xi_2)^T = K \cdot (\varepsilon_1,\varepsilon_2)^T$ has variance $\mathrm{var}(\xi_i) = K^2\mathrm{var}(\varepsilon_i)$, $i = 1,2$, where $\boldsymbol{\varepsilon} = (\varepsilon_1,\varepsilon_2)^T$ is the random noise term in the original nonlinear model. Let $\mathcal{B}$ be the back-shift operator, $\mathcal{B}\boldsymbol{w}(t) = \boldsymbol{w}(t-1)$. Then the model can be written as

$$[I - c(I - dE)\mathcal{B}]\boldsymbol{w} = \boldsymbol{\xi} \quad \text{(B2)}$$

where I is the identity matrix and $E = \begin{bmatrix} 1 & -1 \\ -1 & 1 \end{bmatrix}$.

We define the spectral matrix of the two-dimensional stationary stochastic process $\boldsymbol{y}(t) = (y_1(t),y_2(t))$ as

$$S_{yy} = \begin{bmatrix} S_{y_1y_1} & S_{y_1y_2} \\ S_{y_2y_1} & S_{y_2y_2} \end{bmatrix} \quad \text{(B3)}$$

where $S_{y_1y_1}$, $S_{y_2y_2}$ are the power spectra of y_1 and y_2 respectively, $S_{y_1y_2}$ and $S_{y_2y_1}$ are cross spectra, and $\mathrm{Re}(S_{y_1y_2}) = \mathrm{Re}(S_{y_2y_1})$ is the co-spectrum. These are intended to be the analytically defined spectra and cross spectra of a stationary stochastic process, distinct from the discrete Fourier transform-based estimator of the previous section, though the discrete Fourier transform-based quantity provides statistical estimators of the analytic spectrum under appropriate conditions (Brillinger 2001). Write the autocovariance and cross-autocovariance function of $\boldsymbol{y}(t) = (y_1(t), y_2(t))$ as $\gamma_{kl}(t) = \mathrm{cov}(y_k(s), y_l(s+t))$ where $k,l \in \{1,2\}$. The power spectrum and cospectrum are defined as Fourier transform of autocovariance and cross autocovariance function

$$S_{y_k y_l}(f) = \sum_{t=-\infty}^{\infty} \gamma_{kl}(t) e^{-2\pi i f t}$$

where $k,l \in \{1,2\}$. Note that $S_{y_k y_l}(f) = S_{y_k y_l}(-f)$, we thus only consider $0 < f \leq 1/2$.

Now we will compute the S_{ww} by the same approach in the SI of Deshamais et al. (2018). Computing the spectral matrix of both side of （B2）, we have

$$T S_{ww} \overline{T} = S_{\xi\xi} \tag{B6}$$

where S_{ww} and $S_{\xi\xi}$ are spectral matrices of $\boldsymbol{w}$ and $\boldsymbol{\xi}$ and the matrix T is

$$T = I - c(I - dE)\mu \tag{B7}$$

where $\mu(f) = \exp(-2\pi i f)$, and f is frequency in units of cycles per sampling interval (note the different units from Appendix A). $\overline{T}$ is the conjugate transpose of matrix T. From （B6） and （B7） we have

$$S_{ww} = R S_{\xi\xi} \overline{R} \tag{B8}$$

where $R = T^{-1} = \frac{1}{1-c\mu} I - \frac{1}{1-c\mu} \cdot \frac{cd\mu}{1-c\mu+2cd\mu} E$.

Given the symmetry of the vector time series $\boldsymbol{w} = (w_1, w_2)^T$ and $\boldsymbol{\xi} = (\xi_1, \xi_2)^T$, we can write $S_w = S_{w_1w_1} = S_{w_2w_2}$ as the power spectrum, $C_w = \mathrm{Re}(S_{w_1w_2}) = \mathrm{Re}(S_{w_2w_1})$

as the co-spectrum, and introduce the same notations for $\boldsymbol{\xi}$. From the matrix equation (B8) and the explicit representation of R, we have, after some algebra,

$$\begin{cases} S_w(f) = \left(\dfrac{1}{1+c^2-2cu}\right)(S_\xi - \alpha S_\xi + \alpha C_\xi) \\ C_w(f) = \left(\dfrac{1}{1+c^2-2cu}\right)(C_\xi - \alpha C_\xi + \alpha S_\xi) \end{cases} \tag{B9}$$

where

$$\alpha(f) = \frac{2cd\ \ (-c+cd+u(f))}{(-c+2cd)^2+1+2(-c+2cd)u(f)} \tag{B10}$$

and $u(f) = \cos(2\pi f)$.

We assume that the correlation between the environmental noise ε_1 and ε_2 (and between ξ_1 and ξ_2) is ρ $(0 \le \rho < 1)$ at any frequency, i.e.

$$C_\xi(f) = \rho \cdot S_\xi(f). \tag{B11}$$

Then (B9) can be simplified:

$$\begin{cases} S_w(f) = \left(\dfrac{1}{1+c^2-2cu}\right)[(1-\alpha)+\alpha\rho]S_\xi \\ C_w(f) = \left(\dfrac{1}{1+c^2-2cu}\right)[(1-\alpha)\rho+\alpha]S_\xi. \end{cases} \tag{12}$$

Background information of spectral analysis of time series can be found in Shumway & Stoffer (2017) and Reinsel (1993).

In the following, we will use the timescale σ instead of frequency f. Because, in this section, f is in units of cycles per sampling interval, σ is

$$\sigma = \frac{1}{f}, \tag{B13}$$

and as $0 < f \le 1/2$, the range of timescale is $2 \le \sigma < \infty$. (In the analytical results in Fig. 1, 2 and S3a-f, we only take $2 \le \sigma \le 100$ for plotting.) The local population variability, spatial synchrony and metapopulation variability at timescale σ can then be derived from (B12):

$$V_P(\sigma) = \frac{S_w}{K^2} = \frac{(1-\alpha(\sigma)) + \alpha(\sigma)\rho}{1 + c^2 - 2c \cdot u(\sigma)} \cdot \frac{I_0'(\sigma)}{K^2} \tag{B14}$$

$$\phi(\sigma) = \frac{C_w}{S_w} = \frac{(1-\alpha(\sigma))\rho + \alpha(\sigma)}{(1-\alpha(\sigma)) + \alpha(\sigma)\rho} \tag{B15}$$

$$V_M(\sigma) = \frac{2(S_w + C_w)}{(2K)^2} = \left(\frac{1}{1 + c^2 - 2c \cdot u(\sigma)}\right)\frac{1+\rho}{2} \cdot \frac{I_0'(\sigma)}{K^2} \tag{B16}$$

where $u(\sigma) = \cos(2\pi/\sigma)$, and $I_0'(\sigma) = S_\xi\left(\frac{1}{\sigma}\right) = K^2 S_\epsilon\left(\frac{1}{\sigma}\right) \stackrel{\text{def}}{=} K^2 I_0(\sigma)$ is the timescale specific variability of the linearized environmental noise $\boldsymbol{\xi}$ and $I_0(\sigma)$ is the timescale specific variability of the original environmental noise, $\boldsymbol{\varepsilon}$. When the environmental noise is assumed as Gaussian white noise (we take this assumption all across the paper except the red noise cases in Fig. 4d,h and S7d,h), $I_0(\sigma)$ and $I_0'(\sigma)$ are constant across all timescales.

Relationship of timescale-specific variability and synchrony with dispersal rate $\boldsymbol{d}$, timescale $\boldsymbol{\sigma}$ and environmental synchrony $\boldsymbol{\rho}$

One main finding from the model is that dispersal rate d has different effects on timescale specific variability and synchrony in short and long timescales (Figure 2 and S1). This can be verified from the analytical results of the local linearized model. From (B10) we have

$$\frac{\partial \alpha}{\partial d} = \frac{2(c^2 - 2cu + 1)}{\left((-c + 2cd)^2 + 1 + 2(-c + 2cd)u\right)^2} \cdot c(u - c(1-2d)). \tag{B17}$$

Thus when $c > 0$,

$$\begin{cases} \frac{\partial \alpha}{\partial d} > 0 \Leftrightarrow u = \cos\left(\frac{2\pi}{\sigma}\right) > c(1-2d) \\ \frac{\partial \alpha}{\partial d} < 0 \Leftrightarrow u = \cos\left(\frac{2\pi}{\sigma}\right) < c(1-2d), \end{cases} \tag{B18}$$

where we here rely on a straightforward check that the numerator and denominator of the fraction in (B17) are both positive. When $c < 0$, the results in (B18) inverses. From (B14), (B15) and (B16), we have

$$\frac{\partial V_P}{\partial d} = -\left(\frac{1}{1+c^2-2cu}\right)(1-\rho)I_0 \cdot \frac{\partial \alpha}{\partial d} \quad \text{(B19)}$$

$$\frac{\partial \phi}{\partial d} = \frac{(1-\rho^2)}{[(1-\alpha)+\alpha\rho]^2} \cdot \frac{\partial \alpha}{\partial d} \quad \text{(B20)}$$

$$\frac{\partial V_M}{\partial d} = 0 \quad \text{(B21)}$$

Since $-\left(\frac{1}{1+c^2-2cu}\right)(1-\rho)I_0 < 0$ and $\frac{(1-\rho^2)}{[(1-\alpha)+\alpha\rho]^2} > 0$, we have the following statements: When $0 < r < 1$ (i.e. $0 < c < 1$, under-compensatory), as dispersal rate d increases within the range $(0,0.5)$,

(a.1) local variability V_P decreases at long timescales (i.e. large σ) and increases at short timescales (i.e. small σ);

(a.2) spatial synchrony ϕ increases at long timescales and decreases at short timescales;

(a.3) metapopulation variability V_M is not dependent on d;

(a.4) the bound of short/long timescale is $u = \cos(2\pi/\sigma) = c(1-2d)$.

When $1 < r < 2$ (i.e. $-1 < c < 0$, over-compensatory), all above predictions are reversed.

Then we will investigate the change of timescale-specific variability and synchrony with the change timescale σ, which is equivalent to the change of $u(\sigma) = \cos(2\pi/\sigma)$. From (B16), we know that V_M increases (decreases) with u when $c > 0$ ($c < 0$). Since

$$\frac{\partial \alpha}{\partial u} = \frac{2cd(1+2c^2d-c^2)}{((-c+2cd)^2+1+2(-c+2cd)u)^2} \quad \text{(B22)}$$

and

$$\frac{\partial \phi}{\partial u} = \frac{(1-\rho^2)}{[(1-\alpha)+\alpha\rho]^2} \cdot \frac{\partial \alpha}{\partial u} \quad \text{(B23)}$$

then ϕ increases (decreases) with u when $c > 0$ ($c < 0$) because $(1+2c^2d-c^2) \geq 0$.

The change of V_p with σ is difficult to verify with pencil & paper. Let $\psi = (1 + c^2 - 2cu)^{-1}$, then

$$\frac{1}{I_0} \cdot \frac{\partial V_P}{\partial u} = \frac{\partial}{\partial u}\psi - (1-\rho)\frac{\partial}{\partial u}(\psi\alpha) \tag{B24}$$

When $c > 0$, $\psi\alpha$ increases with u because both ψ and α increases with u, then

$$\frac{\partial}{\partial u}\psi - (1-\rho)\frac{\partial}{\partial u}(\psi\alpha) \geq \frac{\partial}{\partial u}\psi - \frac{\partial}{\partial u}(\psi\alpha) = \frac{\partial}{\partial u}[\psi(1-\alpha)]$$

Let

$$1 - \alpha = \frac{(2cd-c)^2 + 1 + 2(2cd-c)u - 2cd \quad (-c + cd + u)}{(2cd-c)^2 + 1 + 2(2cd-c)u} \stackrel{\text{def}}{=} \frac{A}{B} \tag{B25}$$

Note that

$$\frac{\partial\psi}{\partial u} = \psi \cdot \frac{2c}{1 + c^2 - 2cu} \tag{B26}$$

and from （18）,

$$\frac{\partial(1-\alpha)}{\partial u} = -\frac{\partial\alpha}{\partial u} = -(1-\alpha) \cdot \frac{2cd(1 + 2c^2d - c^2)}{AB} \tag{B25}$$

then

$$\frac{\partial}{\partial u}[\psi(1-\alpha)] = \psi(1-\alpha) \cdot c\left(\frac{2}{1 + c^2 - 2cu} - \frac{2d(1 + 2c^2d - c^2)}{AB}\right) \tag{B26}$$

Then using Matlab (see the code in the last of Appendix B), we can numerically find that

$$\frac{2}{1 + c^2 - 2cu} - \frac{2d(1 + 2c^2d - c^2)}{AB} > 0 \tag{B27}$$

When $c < 0$, ψ and α decreases with u, then $\frac{\partial}{\partial u}(\psi\alpha) < 0$,

$$\frac{\partial}{\partial u}\psi - (1-\rho)\frac{\partial}{\partial u}(\psi\alpha) \leq \frac{\partial}{\partial u}[\psi(1-\alpha)]$$

and from (B26) we know that when $c < 0$, $\frac{\partial}{\partial u}[\psi(1-\alpha)] < 0$.

Since $u(\sigma) = \cos(2\pi/\sigma)$ increases with timescale σ, we can conclude that:

(b) V_M, ϕ and V_M increases (decreases) with σ when $r < 1$ $(r > 1)$.

The change of V_P, ϕ and V_M with the environmental noise synchrony is

$$\frac{\partial V_P}{\partial \rho} = -\left(\frac{1}{1 + c^2 - 2cu}\right)(1-\rho)\alpha I_0' \tag{B28}$$

$$\frac{\partial \phi}{\partial \rho} = \frac{1 - 2\alpha}{[(1-\alpha) + \alpha\rho]^2} \tag{B29}$$

and

$$\frac{\partial V_M}{\partial \rho} = \frac{2}{1 + c^2 - 2cu} I_0' \tag{B30}$$

Note that

$$\frac{\partial V_P}{\partial \rho} < 0 \Leftrightarrow \alpha > 0 \Leftrightarrow 2cd \quad (-c + cd + \cos(2\pi/\sigma)) \quad > 0 \tag{B31}$$

Then we find that:

(c.1) When $r < 1$ $(r > 1)$, V_P increases (decreases) with ρ in long timescale (i.e. $\cos(2\pi/\sigma) < c - cd$) and decrease (increases) with ρ in short timescale.

(c,2) ϕ and V_M always increase with ρ.

(c.3) Timescale-specific Moran's theorem (Desharnais et al. 2018, but in a different model): When $d = 0$, $\alpha = 0$ and $\phi(\sigma) = \rho$.

The sign of timescale-specific synchrony ϕ can be determined as

$$\phi < 0 \Leftrightarrow (1-\alpha)\rho + \alpha < 0 \Leftrightarrow \alpha < 1 - \frac{1}{1-\rho} \tag{B32}$$

and when $\rho = 0$, $\phi < 0$ when

$$c \left(-c + cd + \cos\left(\frac{2\pi}{\sigma}\right)\right) \quad < 0 \tag{B33}$$

Matlab code to verify (27):

u=[0.99:-0.01:-0.99];

```
c=[0.01:0.01:0.99];
d=[0.01:0.01:0.49];
for i=1:199
    for j=1:99
        for k=1:49
            A=(c(j)-2*c(j)*d(k))^2+1+2*(c(j)*d(k)-c(j))*u(i)-
2*c(j)*d(k)*(c(j)*d(k)-c(j));
            B=(2*c(j)*d(k)-c(j))^2+1+2*(2*c(j)*d(k)-c(j))*u(i);
            Psi=2/(1+c(j)^2-2*c(j)*u(i));
            E=2*d(k)*(1+2*c(j)^2*d(k)-c(j)^2);
            F(i,j,k)=Psi-E/(A*B);
        end
    end
end
m=min(min(min(F))); %m=0.1364
```

Reference

Bloomfield, P., 2004. Fourier analysis of time series: an introduction. John Wiley & Sons. New York.

Brillinger, D. R., 2001. Time series: data analysis and theory. Society for Industrial and Applied Mathematics. San Francisco.

Desharnais, R. A., D. C. Reuman, R. F. Costantino, and J. E. Cohen. 2018. Temporal scale of environmental correlations affects ecological synchrony. Ecology Letters 21: 1800–1811.

Murray, J. D. 2002. Mathematical biology, 3rd ed. Interdisciplinary applied mathematics. Springer, New York.

Reinsel, G. C. 1993. Elements of Multivariate Time Series Analysis, Springer Series in Statistics. Springer US, New York, NY.

Shumway, R. H., and D. S. Stoffer. 2017. Time Series Analysis and Its Applications: With R Examples, Springer Texts in Statistics. Springer International Publishing, Cham.

Wang, S., B. Haegeman, B., and M. Loreau. 2015. Dispersal and metapopulation stability. PeerJ 3: e1295.

Appendix C. Determining the critical length of time series in metapopulations

In the main text, we show that time series length has a significant impact on the relationship between dispersal and population variability, and short time series may reveal unexpected relationships that are in contrast to theoretical expectations. Here we conduct simulations to determine a tentative time series length for obtaining an empirical relationship that is consistent with theoretical expectation.

We simulate metapopulation dynamics with parameters: $r = 0.5,\ \rho = 0.4,\ d = [0, 0.05, 0.1, 0.15]$. We perform $N = 1, 2, ..., 10$ paralleled simulations, mimicking the number of replicates in experimental studies. We choose $\rho = 0.4$ to introduce spatial correlation in environmental fluctuations, which is same among all pair of time series, either between the two patches within one metapopulation replicate or among N replicates. We simulated four rates of dispersal, considering most metapopulation experiments have up to four dispersal gradients (no, low, intermediate, high dispersal). Our simulations were designed to match experimental settings.

Given a "pre-assigned time series length" L, we calculated spatial synchrony from simulated time series and then examine the relationship between spatial synchrony and dispersal (Fig. C1). We use a linear regression to test whether they exhibit a significant (p-value<0.05, obtained by two-side t-test) and positive relationship between dispersal rate and (overall) spatial synchrony. When there are more replicates, we calculate spatial synchrony for each replicate and the statistical test was performed by combining data from all replicates. For example, in Fig. C1 left, there is one replicate so we have one value of synchrony calculated under each dispersal rate, and in Fig. C1 right, there are six replicates so we have six values of synchrony calculated under each dispersal rate. When calculating the critical length, we repeat these processes for 2000 times and calculate the accuracy, i.e. the fraction that a significant positive relationship is obtained. We then change the "pre-assigned time series length" L and determine the critical length that lead to an accuracy of 50% or 80% (for example, see Fig. C2). Figure C3 shows the derived critical time series length under various conditions to obtain significant (p-value > 0.05) positive relationships between dispersal and spatial

synchrony.

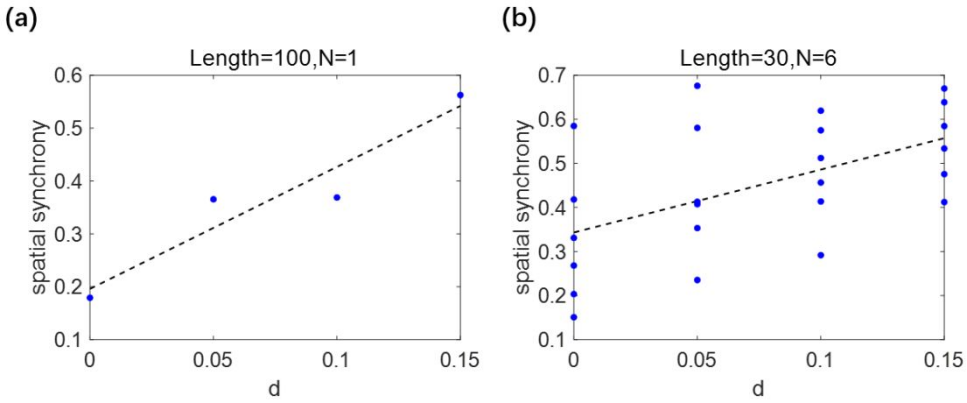

Figure C1. An example of resulting relationship between dispersal and spatial synchrony, blue points are the spatial synchrony under different dispersal rate calculated from simulation and dash lines are the linear regression lines. Left: $N = 1,\ L = 100$; Right: $N = 6, L = 30$. Parameters: $r = 0.5,\ \rho = 0.4,\ K = 10,$ var $(\epsilon) = 0.1$. The dashed lines show regression lines. In this example the regression coefficients are both positive and significant.

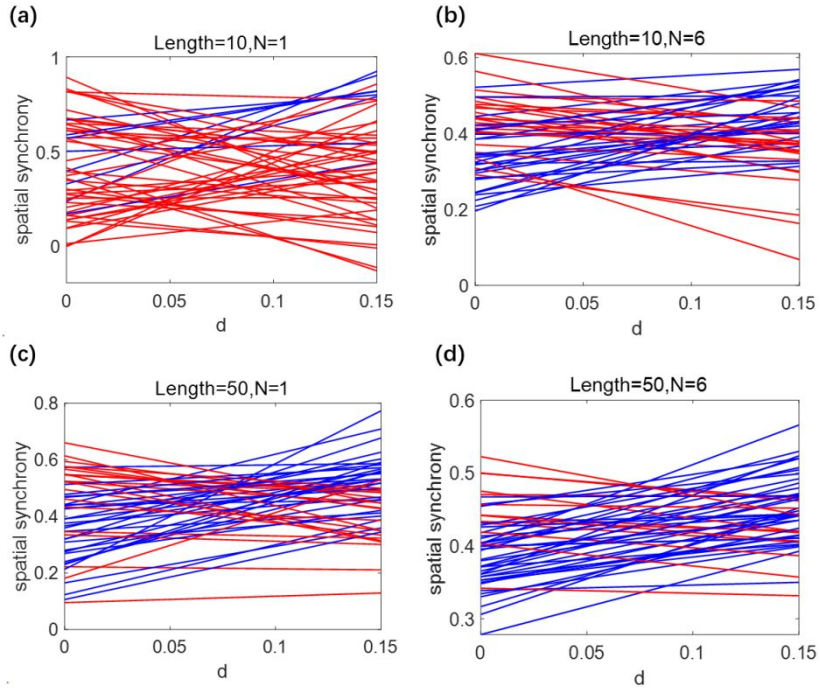

Figure C2. 50 independent least squared regression lines of spatial synchrony with dispersal rate $d = 0,0.05,0.1,0.15$, time length is 10 (a,b) and 50 (c,d). 1 (a,c) and 6 (b,d) replications. Parameters: $r = 0.5,\ \rho = 0.4\ \ K = 10,$ var$(\epsilon) = 0.1$. The

regression lines are blue when the effect of dispersal on spatial synchrony is significant (p-value<0.05) and positive. Otherwise the lines are red. The proportions of blue lines (i.e. the "success rate") in scenarios (a) to (d) are respectively 16%, 52%, 58%, 74%.

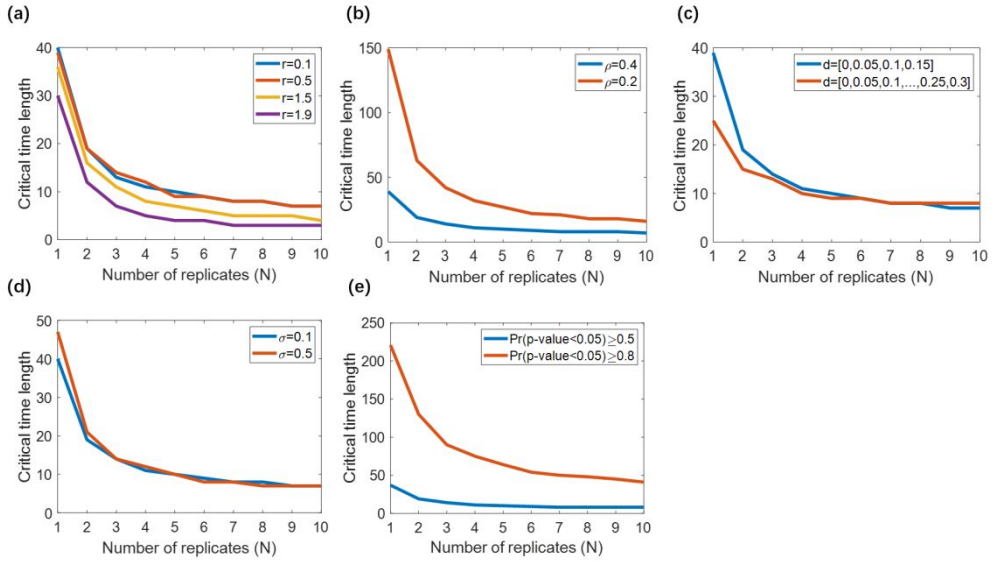

Figure C3. The critical time series length required for obtaining the theoretical expected relationship between dispersal and spatial synchrony with probability 0.5 (probability of obtaining significant negative relationship, p-value<0.05), as a function of the number of replicates N. When not specified, the parameters are $r = 0.5$, $d = [0,0.05,0.1,0.15]$, $\rho = 0.4$, $K = 10$, $\mathrm{var}(\epsilon) = 0.1$. The probability of obtaining expected relationship is calculated by the proportion in 2000 simulated communities. (a) Effect of growth rate. (b) Effect of environmental synchrony. (c) Effect of dispersal gradient. (d) Effect of variance of environmental noise. (e) Suggested critical length with different demands of accuracy.

Appendix D. Supplementary Figures.

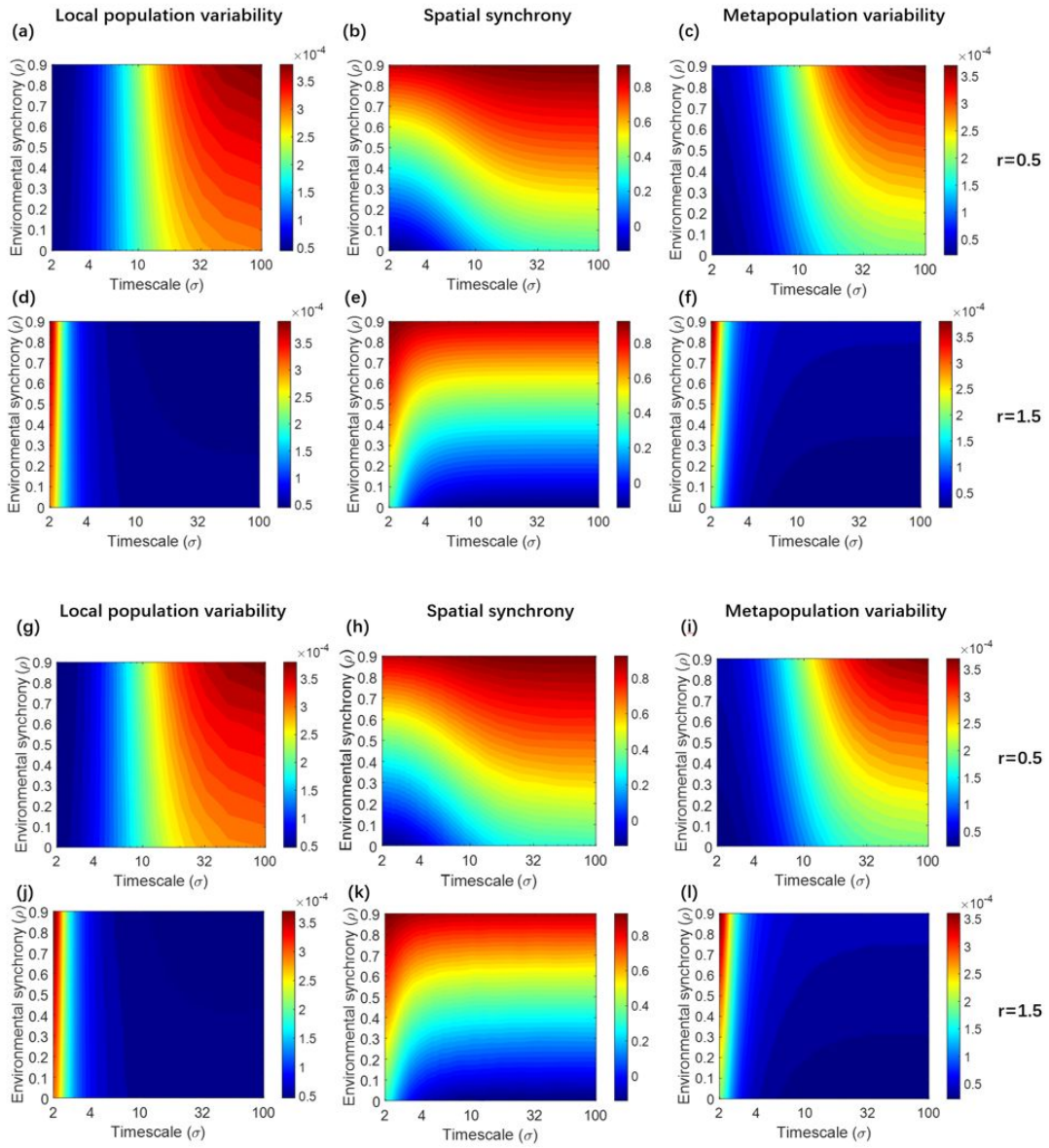

Figure D1. The effect of environmental synchrony (ρ) on timescale-specific local population variability (a,d), spatial synchrony (b,e), and metapopulation variability (c,f), in under- (a,b,c,g,h,i) and over-compensatory systems (d,e,f,j,k,l). Results are obtained from analytical approximations (a,b,c,d,e,f) and simulation of original nonlinear model (g,h,i,j,k,l). Parameters: $d = 0.2, K = 10,$ $\mathrm{var}(\epsilon) = 0.01$, time length=200. The results represent the average values across 5000 simulated communities.

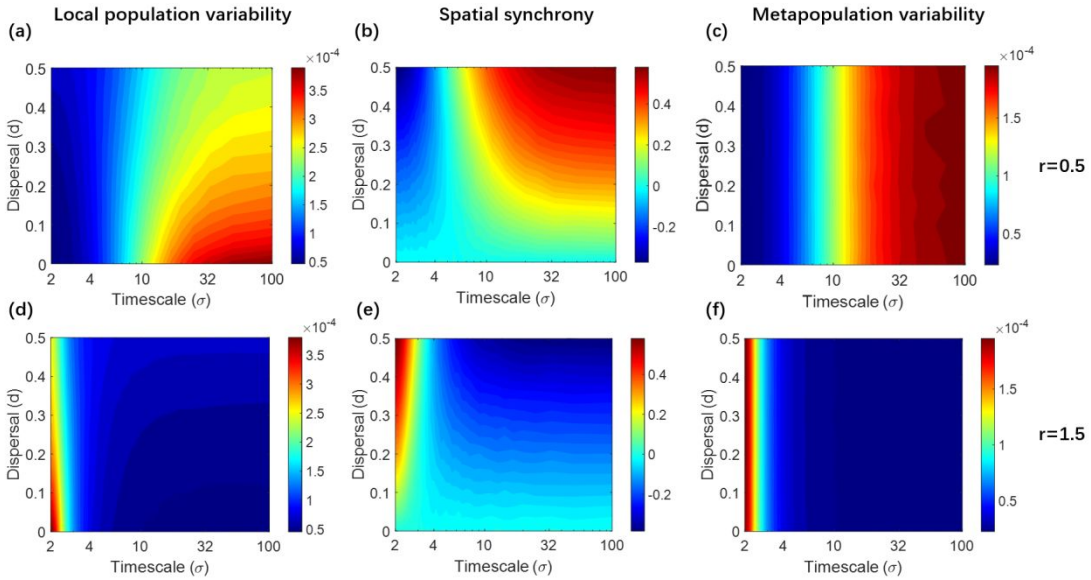

Figure D2. The effect of dispersal (d) on timescale-specific local population variability (a,d), spatial synchrony (b,e), and metapopulation variability (c,f), in under- (a,b,c) and over-compensatory systems (d,e,f). Parameters: $\rho = 0, K = 10,$ var(ϵ) $= 0.01,$ time length=200. The results represent the average values across 5000 simulated communities.

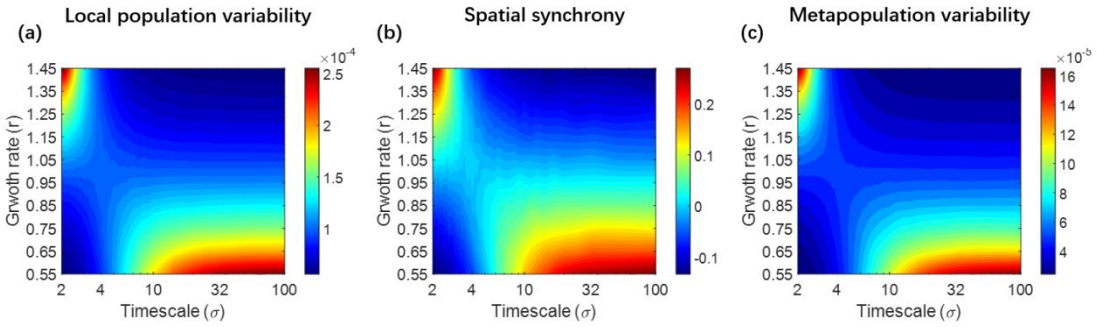

Figure D3. The effect of intrinsic growth rate (r) on timescale-specific local population variability (a), spatial synchrony (b), and metapopulation variability (c). Parameters: $\rho = 0, d = 0.2, K = 10$, $\mathrm{var}(\epsilon) = 0.01$, time length=200. The simulation results represent the average values across 5000 simulated communities.

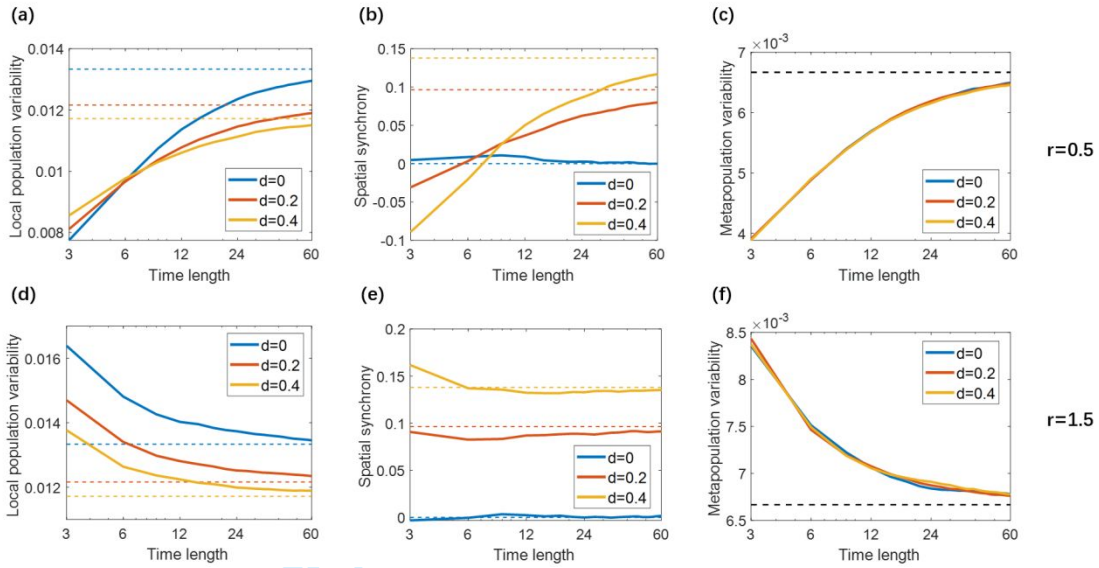

Figure D4. The effect of time series length on sample estimate of local population variability (a,d), spatial synchrony (b,e) and metapopulation variability (c,f) in under- (a,b,c) and over-compensatory systems (d,e,f). The solid lines show the overall variabilities and synchronies calculated from simulation (blue, red, yellow: $d = 0, 0.2, 0.4$) and dash lines show the theoretical variabilities and synchronies (Wang et al. 2015). Parameters: $\rho = 0$, $\mathrm{var}(\epsilon) = 0.01$, $K = 10$. Time series length = 3 ~ 60. The results represent the average across 10000 simulated communities.

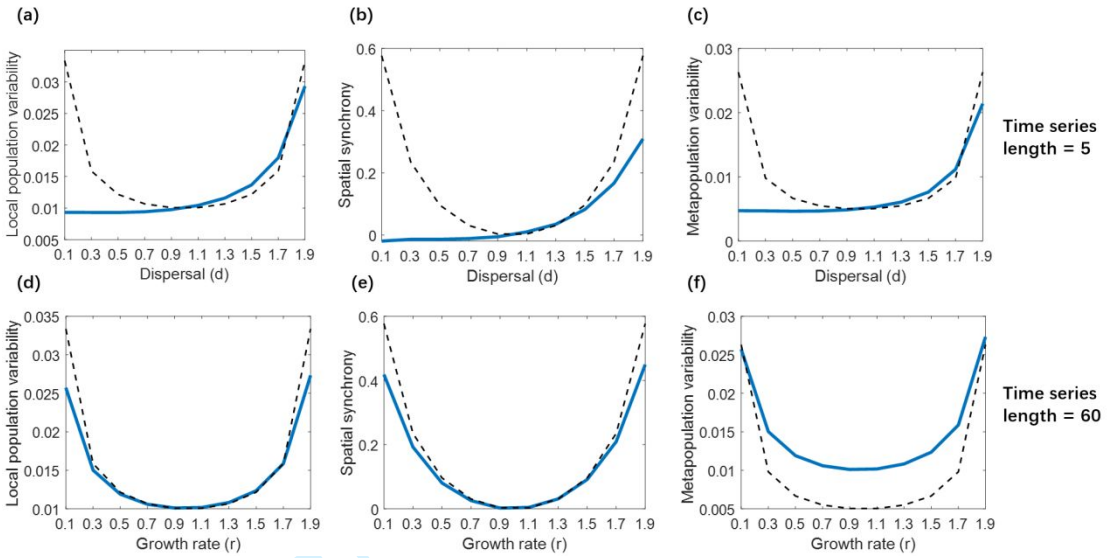

Figure D5. Effect of intrinsic growth rate (r) on local population variability (a,c) and spatial synchrony (b,d) calculated from short (5) and long (60) time series. Solid lines: results calculated from finite long time series. Dashes lines: analytical results (stationary variability and synchrony, from Wang (2015)). Parameters: $\rho = 0$, $d = 0.2$, $K = 10$, $\mathrm{var}(\epsilon) = 0.01$. The results represent the average across 500000 (length=5) or 50000 (length=60) simulated communities.

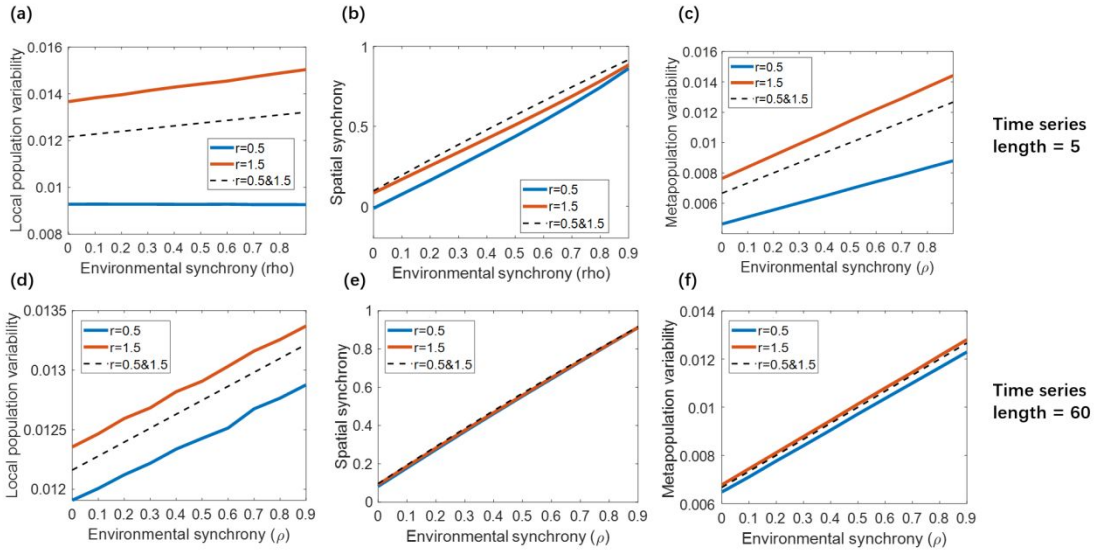

Figure D6. Effect of intrinsic growth rate (r) on local population variability (a,c) and spatial synchrony (b,d) calculated from short (5) and long (60) time series. Solid lines: results calculated from finite long time series, $r = 0.5$ (blue) and 1.5 (red). Dashes lines: analytical results (stationary variability and synchrony, from Wang (2015), same for $r = 0.5$ and 1.5). Parameters: $d = 0.2$, $K = 10$, $\mathrm{var}(\epsilon) = 0.01$. The results represent the average across 500000 (length=5) or 50000 (length=60) simulated communities.

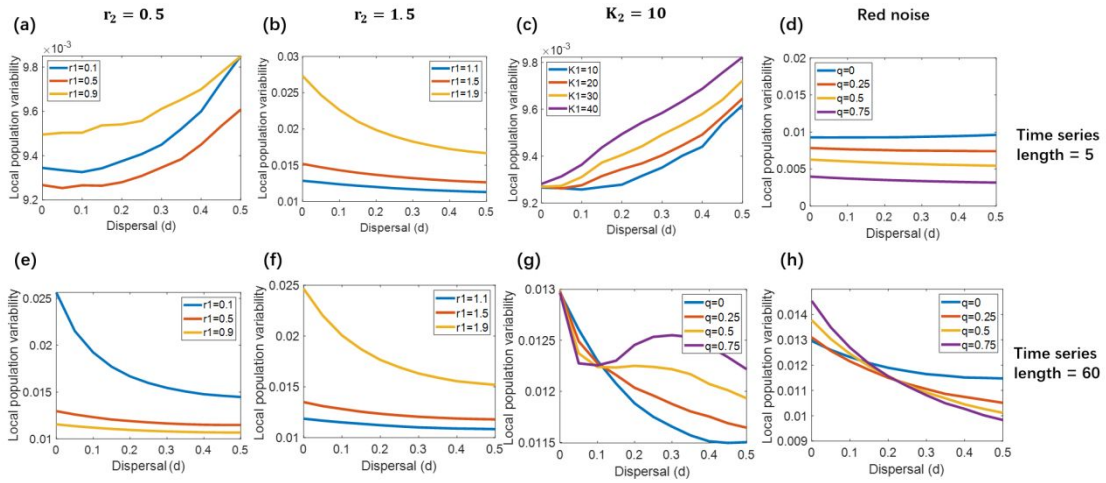

Figure D7. Effect of dispersal on local population variability calculated from short (a,b,c,d), and long (e,f,g,h) time series under four scenarios: spatial heterogeneity in the intrinsic rate of under-compensatory grown (a,e), spatial heterogeneity in the intrinsic rate of over-compensatory grown (b,f), spatial heterogeneity in the carrying capacity (c,g), and temporally autocorrelated environmental noise (i.e. red noise; d,h). Parameters are set as follows when not specified: $\rho = 0$, $\mathrm{var}(\epsilon) = 0.1$, $\mathrm{r} = 0.5$ $K = 10$. The results represent the average across 500000 (length=5) or 50000 (length=60) simulated communities.

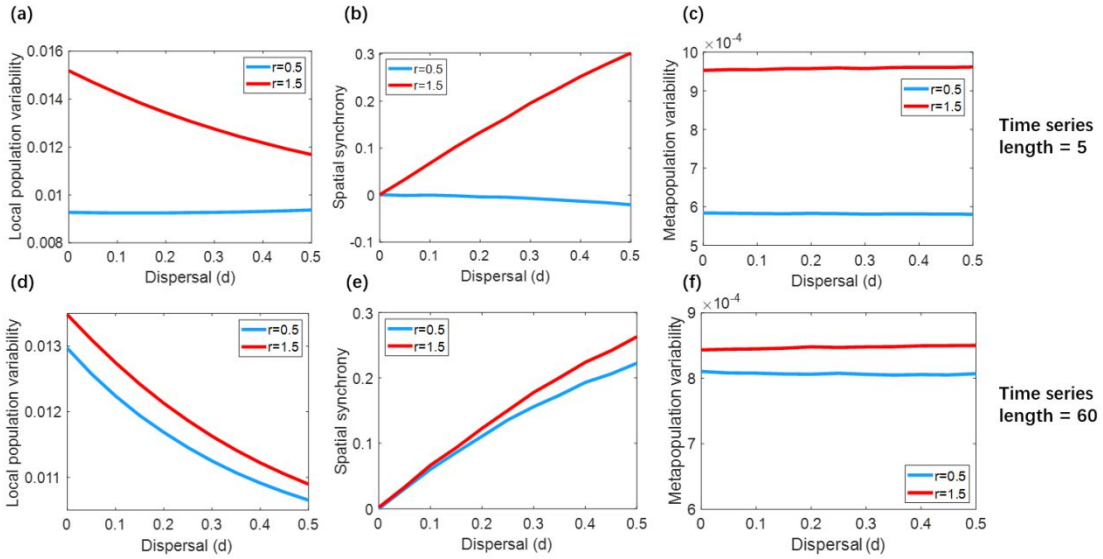

Figure D8. Effect of dispersal on spatial synchrony calculated from short (a,b,c,d), and long (e,f,g,h) time series, based on a 16-patch metapopulation model with global dispersal. Blue and red lines represent models with under- and over-compensatory population growth ($r = 0.5$ or 1.5), respectively. Parameters: $\rho = 0$, var $(\epsilon) = 0.1$, $K = 10$. The results represent the average across 500000 (length=5) or 50000 (length=60) simulated communities.